PHYSICAL REVIEW LETTERS

Towards Bose-Einstein Condensation of Semiconductor Excitons: The Biexciton Polarization Effect

D. Hägele,* S. Pfalz, and M. Oestreich

Institut für Festkörperphysik, Leibniz Universität Hannover, Appelstraße 2, D-30167 Hannover, Germany

We theoretically predict a strong influence of stimulated exciton-exciton scattering on semiconductor luminescence. The stimulated scattering causes circularly polarized instead of unpolarized emission at the biexciton emission line in a degenerate gas of partly spin polarized excitons. The biexciton polarization effect increases with increasing exciton densities and decreasing temperatures and approaches almost unity in the ultimate case of Bose-Einstein condensation. Time- and polarization-resolved luminescence measurements evidence the biexciton polarization effect both in ZnSe and GaAs quantum wells.

Bose-Einstein condensation (BEC) in atoms is now routinely validated by a set of measurable effects like the velocity distribution of the atoms [1] or more advanced coherence effects [2]. Proving BEC of bound electron hole pairs—so-called excitons—in semiconductors is in a way more challenging, although the BEC transition temperatures for excitons can be many orders of magnitude higher than in atoms. In 1962 Blatt, Böer, and Brandt predicted that optically created excitons in semiconductors undergo Bose-Einstein condensation at sufficiently high densities and low temperatures [3]. The critical temperature for condensation, $T_c \propto n^{2/3}m^{-1}$, depends on particle density n and the effective exciton mass m. Compared to atoms, T_c in semiconductors is about 8 orders of magnitude higher, where the lower effective exciton mass contributes about 5 orders and the higher achievable exciton densities about 3 orders. The resulting T_c's in common semiconductors can be as high as a few kelvins. Blatt, Böer, and Brandt suggested already in their pioneering work a narrowing of the homogeneous photoluminescence (PL) linewidth as a signature of BEC that is caused by the absence of exciton scattering within the condensate. This criterion, however, cannot be applied to most semiconductors, especially the prominent candidates Cu_2O and CuCl, as their inhomogeneous linewidths, which are caused by strain, are generally larger than the homogeneous linewidth [4]. Alternatively, Fernández-Rossier, Tejedor, and Merlin suggested measuring the photon statistics of PL from a condensate which should exhibit nonthermal laserlike behavior [5]. Detection of such signatures, however, does require sophisticated quantum optical methods. A number of interesting effects towards BEC have been found in coupled quantum wells [6]. However, their interpretation is "notoriously complex," as stated in Ref. [7]. BEC of excitons has to be contrasted with BEC of polaritons in semiconductor microcavities which has recently grown into a mature field [8]. Unlike in the present Letter, the strong exciton light coupling is a vital prerequisite for condensation which results in the exciting phenomenon of spatial coherence and non-

linear enhancement of circular polarized light emission even far below the laser threshold [9,10].

In the following we numerically find a novel effect in the luminescence of a gas of partly spin polarized semiconductor excitons. The degree of circular polarization of light emitted from bound pairs of excitons with opposite spins (so-called biexcitons [11]) turns from zero to finite at low temperatures and high exciton densities. This biexciton polarization effect (BPE) challenges intuition as biexcitons possess zero total spin. We analytically show that the BPE has its origin in stimulated scattering of excitons reaching its maximum in the case of BEC. First experiments in ZnSe and GaAs quantum wells (QWs) exhibit an onset of a 5% BPE at a sample temperature of 10 K and elevated exciton densities in accordance with theory. The following treatment of semiconductor luminescence complements existing theories [12,13], as it is based on simple assumptions, includes multi-exciton effects, accounts for the exciton spin structure, and allows for the calculation of PL spectra at finite temperatures. Choosing the QW growth direction z as the quantization direction, conduction band electrons with spin $+1/2$ and $-1/2$ and heavy holes in the valence band with spin $+3/2$ and $-3/2$ form exciton states with total spin $+2$, $+1$, -1, and -2. We regard only optically active excitons with spin ± 1 in the $1s$ state in the model and neglect the so-called dark excitons with spin ± 2 and higher excited states. A justification will be given below. The one-dimensional model consists of N adjacent sites in configuration space with a distance of one exciton diameter. The annihilation operators are given by $X_{j,s}$ for an exciton at site j with spin $s = \pm 1$ in the site representation and by $x_{k,s} = N^{-1/2}\sum_j X_{j,s} \exp[2\pi i(kj/N)]$ in the momentum representation. The model Hamiltonian

$$H = \sum_{k,s=\pm 1} E_k x_{k,s}^\dagger x_{k,s} + \sum_j V_B X_{j,+1}^\dagger X_{j,+1} X_{j,-1}^\dagger X_{j,-1}$$

includes the dispersion relation E_k for excitons and an on-site binding potential $V_B < 0$ for biexciton formation (for a very similar Hamiltonian see Ref. [14]). The operator

146402-1

commutation relations were chosen to exhibit both bosonic and fermionic properties $X_{j,s}X_{l,s} = X_{l,s}X_{j,s}$ and $X_{j,s}^2 = 0$, respectively. The second relation regards the fact that due to Pauli blocking no more than one exciton with spin s may occupy a certain site (hard-core bosons). The on-site potential reflects the fact that formation of biexcitons is (like the formation of the H_2 molecule) governed by short range exchange interaction. A coexistence of bright and dark excitons in close spatial vicinity is energetically not favorable because Pauli exclusion—mediated by either electrons or holes with equal spins—leads to lateral confinement which increases kinetic energy. The $2s$, $2p$, . . . states of excitons are also energetically unfavorable. The above model with $1s$ excitons of spin $s = \pm 1$ captures therefore the physics of the regions with optically active excitons at moderate to low temperatures.

Photoluminescence spectra are calculated numerically using the above Hamiltonian for $N = 7$, where $k = -3, -2, \ldots, 3$, $E_k/\text{eV} = 2.8 + 0.011\{k/[(N+1)/2]\}^2$, and $V_B = -8$ meV mimic the parameters for a ZnSe quantum well [15]. The polarization dependent PL spectra are obtained from

$$I_s(\epsilon) = \sum_{i,f} \langle \psi_i | \rho | \psi_i \rangle |\langle \psi_f | D_s | \psi_i \rangle|^2 \lambda[\epsilon - (\epsilon_i - \epsilon_f)], \quad (1)$$

where $\rho \propto \exp[-(H - \mu_1 n_1 - \mu_{-1} n_{-1})/(k_B T)]$ is the density matrix, μ_1 and μ_{-1} are the chemical potentials for spin ± 1 excitons, the operator $n_s = \sum_j X_{j,s}^\dagger X_{j,s}$ counts the number of excitons with spin s, and $D_s = d\sum_j X_{j,s}$ is the dipole operator in rotating wave approximation that couples to light with angular momentum $s = \pm 1$ (circular polarization). The double sum runs over all 2^{14} multi-exciton eigenstates $|\psi_i\rangle$ and $|\psi_f\rangle$ which were obtained from exact numerical diagonalization of H. The energy difference $\epsilon_i - \epsilon_f$ of the initial and final state determines the spectral position of the emission line λ, where a linewidth of 0.33 meV was chosen. The implicit assumption of thermal equilibrium of ρ is justified in GaAs based quantum wells for densities of about 10^{10} cm^{-2} or higher [16] and in ZnSe based quantum wells for about 10^{11} cm^{-2} due to rapid exciton-exciton scattering [17].

Figures 1(a)–1(d) show calculated spectra for varying temperatures, different densities, and a fixed degree of exciton polarization $(\langle n_1 \rangle - \langle n_{-1} \rangle)/(\langle n_1 \rangle + \langle n_{-1} \rangle) = 0.25$. Figure 1(top) depicts the degree of biexciton polarization for temperatures between 3 and 50 K and densities between 0 and 1.6 excitons per site. We indicated the corresponding positions of spectra (a), (b), and (c) in this diagram. All spectra exhibit two distinct features corresponding to the exciton line at high photon energies (about 2.8 eV) and the biexciton line roughly 6 meV below the exciton line. The fine structure of the spectra is caused by the finite size of the model which must be kept small to be numerically feasible. At 30 K and low densities the spectrum exhibits a weak but significant ($|P| = 5\%$) signature of polarized biexciton emission with the sign opposite to
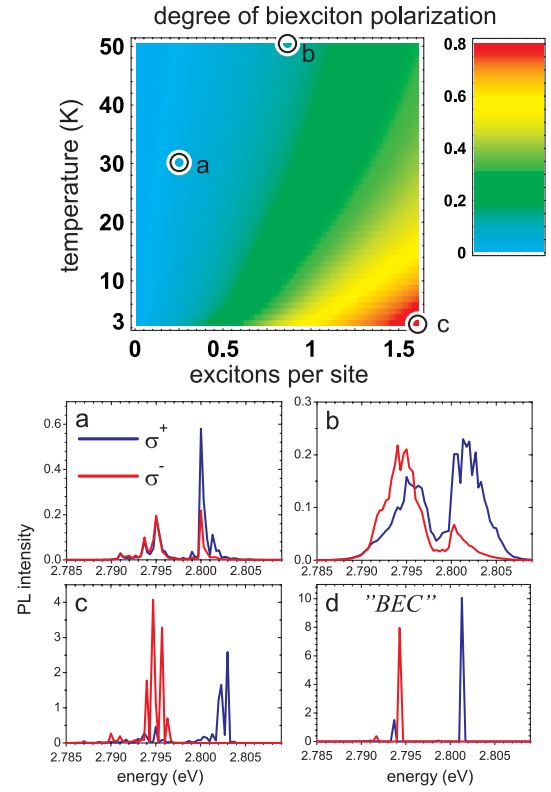

FIG. 1 (color online). (top) Degree of circular polarized biexciton luminescence $|P|$ calculated within the seven site model. (a)–(c) Calculated PL spectra for different points in the temperature-density space (see color plot above). (d) Polarized PL spectrum for $T = 0$ K corresponding to the BEC case with a total of four spin $+1$ and two spin -1 excitons (density of 0.86 excitons per site).

the exciton polarization [Fig. 1(a)]. Increased densities and higher temperatures lead to an expected broadening of both the exciton and biexciton line [Fig. 1(b)]. Approaching the extreme conditions of low temperatures and high densities [Fig. 1(c) and 1(d)], we find three features: (i) the emission lines narrow as predicted by Blatt, Böer, and Brandt [3], (ii) the exciton line shows a blue shift, and (iii) the degree of biexciton polarization reaches an extremum with the sign opposite to the exciton polarization. The exciton line is completely polarized because excitons with opposite spins are bound into the energetically more favorable biexcitons. We conclude from the calculated spectra that apart from narrow spectral lines also a high degree of biexciton polarization is required for the claim of a degenerate exciton gas and ultimately BEC (Kosterlitz-Thouless transition in two dimensions). Increasingly sharp exciton lines can also occur in the limit of low densities at moderate temperatures [Fig. 1(a)] and are therefore not sufficient to prove BEC. In the case of BEC, we moreover expect a sudden and clear appearance of all described spectral features (i) to (iii).

The BPE found in the numerical treatment above will in the following purely analytical discussion be traced back to the bosonic behavior of excitons. The BPE can be com-

pared to stimulated emission of photons where the excitons take on the role of the photons enhancing the optical decay of biexcitons. The influence of the fermionic constituents of the exciton, electron and hole, will be clarified. The temporal derivative of the dipole operator for photons with angular momentum s (Heisenberg picture, no approximations) [15,18]

$$\frac{\hbar}{i}\frac{\partial}{\partial t}D_s = -\left(E_0 D_s + V_B d\sum_j X_{j,-s}^\dagger X_{j,1} X_{j,-1}\right) \quad (2)$$

exhibits one term related to the decay of an exciton and a second term $D_s^{(B)} = d\sum_j X_{j,-s}^\dagger X_{j,1} X_{j,-1}$ where a pair of excitons with opposite spins on the same site is destroyed and an exciton with spin $-s$ is created. This process is known to be the dominant process in biexciton recombination [11]. In thermal equilibrium $D_s^{(B)}$ acts as a stochastic driving term of D_s, which in turn governs the PL. The intensity of the biexciton PL $I_s^{(B)}$ is therefore proportional to the variance (the modulus square) of $D_s^{(B)}$. After introducing the biexciton operator in momentum space $b_{k,s} = N^{-1/2}\sum_j X_{j,1} X_{j,-1} \exp[2\pi i(kj/N)]$, we obtain

$$I_s^{(B)} \propto \langle D_s^{(B)\dagger} D_s^{(B)}\rangle = |d|^2 \sum_{k,k'} \langle b_k^\dagger x_{k,-s} x_{k',-s}^\dagger b_{k'}\rangle$$

$$\approx |d|^2 \sum_k \langle b_k^\dagger x_{k,-s} x_{k,-s}^\dagger b_k\rangle$$

$$= |d|^2 \sum_k \left\langle b_k^\dagger \left(1 + x_{k,-s}^\dagger x_{k,-s} - \frac{2n_s}{N}\right) b_k\right\rangle$$

$$\approx |d|^2 \sum_k \langle b_k^\dagger b_k\rangle \left(1 + \langle x_{k,-s}^\dagger x_{k,-s}\rangle - \frac{2\langle n_s\rangle}{N}\right). \quad (3)$$

The off-diagonal k-dependent contributions disappear in the second line if an incoherent momentum distribution of excitons and biexcitons is assumed. After employing the Bose-like commutation relation in the third line (no approximation, see [15]), we approximate the four operator expectation values by two operator expectation values. We find that the biexciton luminescence intensity depends not only on the occupation of biexcitons $\langle b_k^\dagger b_k\rangle$ as naively expected. The intensity is in fact enhanced by an additional factor $(1 + \langle x_{k,-s}^\dagger x_{k,-s}\rangle - \frac{2\langle n_s\rangle}{N})$ which increases with the occupation $\langle x_{k,-s}^\dagger x_{k,-s}\rangle$ of exciton states. The excitons involved in the enhancement possess the opposite angular momentum as the photons emitted in the biexciton decay. The first two terms of the enhancement factor originate from the bosonic properties of the excitons and correspond to the well-known stimulated-scattering factor "$1 + n$" that appears in stimulated-scattering events in quasi-ideal bosonic systems like lasers or atomic BECs. The bosonic enhancement is counteracted by an additional third term $-2\langle n_s\rangle/N$ which reminds us that an exciton is made of two fermions which are subject to Pauli blocking at high densities [19]. The biexcitonic emissions $I_{+1}^{(B)}$ and $I_{-1}^{(B)}$ are equally strong only if the degree of exciton spin polariza-

tion is zero. If the biexcitons coexist with a majority of spin up (+1) excitons, the spin dependent enhancement factor breaks the symmetry of the biexciton decay channels, resulting in negatively polarized biexciton emission explaining the appearance of the BPE in the calculated spectra. The polarization degree of the BPE $P = (I_1^{(B)} - I_{-1}^{(B)})/(I_1^{(B)} + I_{-1}^{(B)})$ is therefore a natural measure for the deviation from classical towards bosonic behavior of the exciton gas and a key figure in experiments for verifying bosonic behavior of excitons. The biexciton polarization has in a finite model of N sites an upper limit of $|P| < [(N + 1) - 1]/[(N + 1) + 1]$. Complete polarization is expected in large systems, where a macroscopic occupation of the $k = 0$ exciton state appears at low temperatures. Polarized PL of the biexciton will also occur in two- and three-dimensional systems in analogy to the treatment above.

Last we present experimental evidence for the BPE in a single ZnSe QW using time and polarization-resolved PL measurements. Polarization artifacts are excluded by control experiments: (i) changing the sign of the circularly polarized laser pump pulse led to a fully symmetric change in the observed polarized PL, (ii) temporal spin oscillations in an external magnetic field caused oscillations in both the exciton PL polarization and the biexciton PL polarization, (iii) linear polarized laser excitation led to $0 \pm 0.5\%$ circular polarization of the detected PL. The following list of possible effects in the sample reduce the BPE but cannot fake the BPE: (i) reabsorption of light emitted at the
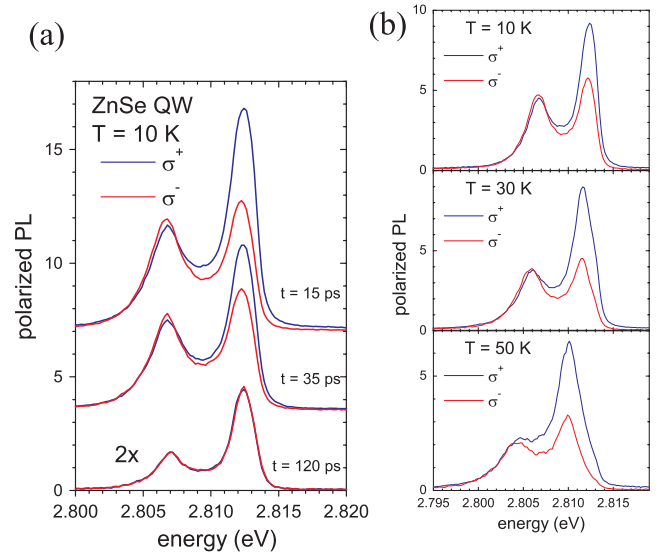

FIG. 2 (color online). (a) Transient, polarization-resolved PL spectra of a 10 nm ZnSe quantum well after resonant pulsed laser excitation. The early spectra exhibit negatively polarized biexciton emission consistently evidencing the biexciton polarization effect. After 120 ps, exciton spin polarization has disappeared (with equal σ^+- and σ^--PL intensity). (b) Polarization-resolved PL spectra for increasing lattice temperatures. The absolute degree of biexciton polarization decreases from 5% at 10 and 30 K to 0% at 50 K.

biexciton line, since the bosonically enhanced decay channel shows stronger reabsorption due to the presence of majority excitons there, (ii) a tiny effect opposite to the BPE, found when we simulated the Purcell effect induced by a polarization dependent refractive index due to bleaching, (iii) biexciton PL superposed by the low energy tail of the polarized exciton PL.

Figure 2 shows PL spectra taken from a 10 nm thick ZnSe QW embedded in 500 nm $ZnS_{0.07}Se_{0.93}$ barriers grown by molecular beam epitaxy on GaAs substrate. Similar data are obtained for an 8 nm ZnSe multiple QW and a 9.9 nm thick GaAs single QW. The ZnSe single QW exhibits large exciton binding energies (>16 meV) and a large heavy-hole light-hole splitting (>25 meV) which makes the system an almost perfect two band semiconductor. A fundamental absorption linewidth of 0.8 meV and a homogeneous linewidth of 0.65 meV measured by four wave mixing spectroscopy demonstrate that disorder is negligible [20]. Excitons with spin $+1$ are created in the sample by circularly polarized ps pulses from a frequency doubled 80 MHz Ti:sapphire laser. The sample is kept at temperatures between 10 and 50 K. The laser energy is tuned to the high energy tail of the heavy-hole resonance to resonantly create a cold exciton gas and reduce stray light at the heavy-hole PL line. The left and right circularly polarized PL components are detected by a spectrometer and a streak camera system with a spectral and temporal resolution of 2 meV and 6 ps, respectively. The setup reaches a polarization sensitivity of 0.5% using an electrically switchable liquid crystal retarder before the polarizer and streak camera.

Spin -1 excitons appear due to rapid spin relaxation already a few ps after excitation, giving rise to the formation of biexcitons from pairs of excitons with opposite spins. Excitons and biexcitons then coexist in a dynamic quasiequilibrium until all carriers decay by optical recombination on a time scale of typically less than 0.5 ns. Figure 2(a) displays polarization-resolved PL spectra 15, 35, and 120 ps after laser excitation. The exciton density of about 10^{11} cm^{-2} is well below the Mott density. At that density thermal equilibrium is always established, allowing for comparison of experiment with theory (see above). The exciton PL exhibits at early times a high degree of circular polarization since the majority of excitons have spin $+1$. Most importantly, the biexciton emission exhibits a significant degree of polarization of about -5% at $t = 15$ ps that has the opposite sign compared to the exciton PL polarization in agreement with the predicted BPE. A higher degree of biexciton polarization would require lower carrier temperatures. Those cannot be obtained in our experiment, because the binding energy that must be dissipated in the biexciton formation process heats the distribution of excitons above lattice temperature. We find completely unpolarized spectra 120 ps after laser excitation when the carrier spin has completely relaxed. We also observe the disappearance of polarized biexciton PL at elevated temperatures and fixed densities which is predicted for the BPE by

our numerics. Figure 2(b) shows the polarization-resolved PL spectra taken 15 ps after laser excitation at 10, 30, and 50 K sample temperature. The spectra at 10 and 30 K clearly exhibit the signature of the BPE. The biexciton polarization at 50 K seems to have reversed the sign, but a line fit which filters out the contribution of the exciton line reveals that the true biexciton polarization is zero within the error bars. A prospective experimental proof of BEC will require lower carrier temperatures that may be obtained by simultaneous creation of excitons and biexcitons via spectrally shaped laser pulses which avoids heating of the exciton gas via the biexciton formation process.

In conclusion, we presented the biexciton polarization effect as a novel signature for bosonic behavior. Our findings contribute to the long-standing question of stimulated exciton scattering and BEC in semiconductors. Photoluminescence experiments verify the existence of the biexciton polarization effect both in ZnSe and GaAs quantum wells.

*Present address: Fakultät für Physik und Astronomie, Ruhr-Universität Bochum, D-44780 Bochum, Germany.

[1] M. H. Anderson *et al.*, Science **269**, 198 (1995).

[2] M. R. Andrews *et al.*, Science **275**, 637 (1997).

[3] J. M. Blatt, K. W. Böer, and W. Brandt, Phys. Rev. **126**, 1691 (1962).

[4] G. Dasbach *et al.*, Phys. Rev. B **70**, 045206 (2004).

[5] J. Fernández-Rossier, C. Tejedor, and R. Merlin, Solid State Commun. **108**, 473 (1998).

[6] D. Snoke, Science **298**, 1368 (2002).

[7] R. Rapaport and G. Chen, J. Phys. Condens. Matter **19**, 295 207 (2007).

[8] D. Snoke, Nature Phys. **4**, 674 (2008).

[9] J. Kasprzak *et al.*, Nature (London) **443**, 409 (2006).

[10] H. T. Cao, T. D. Doan, D. B. Tran Thoai, and H. Haug, Phys. Rev. B **77**, 075320 (2008).

[11] J. C. Kim, D. R. Wake, and J. P. Wolfe, Phys. Rev. B **50**, 15 099 (1994).

[12] M. Kira, F. Jahnke, W. Hoyer, and S. W. Koch, Prog. Quantum Electron. **23**, 189 (1999).

[13] K. Hannewald, S. Glutsch, and F. Bechstedt, Phys. Rev. B **62**, 4519 (2000).

[14] V. M. Agranovich and S. Mukamel, Phys. Lett. A **147**, 155 (1990).

[15] See EPAPS Document No. E-PRLTAO-103-036938 for supplementary material containing detailed derivations. For more information on EPAPS, see http://www.aip.org/pubservs/epaps.html.

[16] R. A. Kaindl, D. Hägele, M. A. Carnahan, and D. S. Chemla, Phys. Rev. B **79**, 045320 (2009).

[17] H. Kalt *et al.*, Phys. Status Solidi B **206**, 103 (1998).

[18] W. Schäfer *et al.*, Phys. Rev. B **53**, 16429 (1996).

[19] H. Haug and S. Schmitt-Rink, Prog. Quantum Electron. **9**, 3 (1984).

[20] T. Voß, Ph.D. thesis, Universität Bremen, 2004.